Journal of Engineering, Project, and Production Management
2026, 16(3), 2026-177

Structural Optimization and Performance Evaluation of Steel Rolling Dies Using Topology Optimization

Tao Chen
Associate Professor, Automotive College, Sanmenxia Polytechnic, Sanmenxia, 472000, China, E-mail: smxct6607@126.com

Engineering Management
Received February 3, 2026; revised March 31, 2026; accepted May 6, 2026
Available online May 29, 2026

Abstract: To address the issues of structural redundancy, stress concentration, and uneven thermal deformation in key components of steel rolling dies under high-load conditions, a coordinated topology optimization-based structural design method for the upper die and slider is proposed. Based on the conventional topology optimization framework, multiple constraints, including volume fraction, stress, deformation, and material distribution, are incorporated. Meanwhile, both impact loading and uniform static loading conditions are considered to establish a unified multi-condition optimization model, enabling the coordinated improvement of structural lightweight design and mechanical performance. Finite element simulations are conducted to compare the structural performance before and after optimization in terms of specific energy absorption, maximum equivalent stress, natural frequency, energy dissipation rate, and deformation uniformity. The results show that the optimized structure achieves up to a 19.6% increase in specific energy absorption and a 29.4% reduction in maximum equivalent stress, while the average natural frequency and energy dissipation rate are improved by 13.2% and 26.3%, respectively. Thermal analysis further indicates that the temperature rise is effectively controlled under different loading conditions, demonstrating good thermal stability. The results confirm that the proposed method can achieve coordinated optimization and performance enhancement of key components under multi-condition constraints, providing practical guidance for the engineering design and optimization of steel rolling dies.

Keywords: Topology optimization, steel rolling dies, structural design, impact load, multi-condition simulation.

DOI 10.32738/JEPPM-2026-177

1. Introduction

Steel rolling dies are key forming tools in the metal rolling process, and their structural design and mechanical properties directly affect the accuracy, surface quality, and production efficiency of the rolled products (You et al. 2023). With the widespread application of high-performance steel and complex alloy sheets, steel rolling dies face higher risks of load, thermal deformation, and fatigue damage during use. Failure may lead to production interruptions and economic losses (Gao et al. 2024; Patwari et al. 2024). However, due to the high strength, low ductility, and brittle characteristics of high-strength steel materials, traditional die design methods are difficult to achieve lightweight and material savings while ensuring mold strength (Elmoghazy et al. 2023). How to conduct structural analysis and material optimization of steel rolling dies to improve their performance has gradually become a focus of research in this field. Zhang et al. (2023) proposed a vibration prediction model based on eXtreme Gradient Boosting (XGBoost) and Bayesian optimization to artificially predict rolling mill vibration and improve rolling process stability. The experimental results showed that the model was superior to existing methods in terms of prediction accuracy, computational efficiency, and stability, and could quantify the influence of various process parameters on vibration. Hu et al. (2024) proposed a virtual debugging framework for dies based on digital twins to address die system vibration in steel rolling production. Research showed that this model could effectively reduce die system vibration and improve utilization of production data and rolling process stability through real-time process parameter optimization. Asadi et al. (2023) proposed an optimization method based on material performance evaluation to address the issues of energy consumption and material damage in the continuous rolling process of steel rolling systems. The study constructed damage criteria for different types of steel and validated them through numerical simulations. The results showed that this method could reduce mold energy consumption and material damage while ensuring material quality. Chen et al. (2023) proposed a roller profile optimization method that combines a density clustering algorithm with a non-dominated sorting genetic algorithm to address roller saturation, high rolling contact pressure, and difficulty in adjusting flatness during continuous cold-rolling mill operation. The research results showed that this method could effectively reduce the rolling gap,

alleviate the contact pressure of the rolling mill rolls, and significantly improve the flatness of the steel rolling die system and reduce the bending force of the working rolls in industrial experiments.

The methods of structural optimization include size optimization, shape optimization, and Topology Optimization (TO). TO is a structural optimization method based on mathematical modeling and numerical iteration, aimed at optimizing the overall layout and connection methods of the structure (Ooms et al. 2023). Compared to size optimization and shape optimization, TO can automatically allocate materials under given constraints, achieving optimal structural performance indicators such as stiffness, strength, and stability (Li et al. 2023). Therefore, in recent years, TO has become the mainstream optimization method and has been widely applied in mechanical structures and mold design. Wang et al. (2024) proposed a multi-material active structure TO method based on the density method, which synergistically distributes active and passive materials in the optimization process to minimize energy consumption and greenhouse gas emissions while satisfying displacement constraints. The research results showed that this method not only significantly reduced structural weight, but also effectively reduced energy consumption and emissions, demonstrating its application prospects in the field of green manufacturing. Banh et al. (2024) proposed an innovative method combining Darcy's law and density method model to address the coupling problem of thermal fluid pressure in TO. The results of numerical examples verified the effectiveness and robustness of this method in dealing with complex coupled problems Zong et al. (2024) combined additive manufacturing and TO technology to design a lightweight quadruped robot limb actuator, reducing its weight by 24.5% and improving its response speed and motion performance, verifying the potential application of TO algorithm in complex motion structures. Frederiksen et al. (2024) proposed an improved strategy based on the third medium contact method to address the challenge of modeling internal contacts in TO. The numerical results showed that this method could effectively improve the stability and feasibility of contact structures under large deformation conditions.

In summary, although existing studies on steel-rolling die design have achieved certain progress in structural optimization and performance improvement, most focus on roll profile or local parameter adjustments, lacking a systematic coordinated optimization approach for key components. As a result, it is difficult to achieve overall structural performance improvement under multi-condition and complex loading scenarios. In addition, insufficient consideration of the coupling effects of multiple constraints and the coordinated design of key components further limits the engineering applicability of current optimization methods. Based on these limitations, this study focuses on the following research questions: how to achieve coordinated optimization of structural lightweight design and mechanical performance under multi-loading conditions such as impact and uniform static loads, and how to realize coordinated optimization of key components of steel-rolling dies under multiple constraints, including volume fraction, stress, and deformation, to enhance overall structural performance and stability. To address these issues, a TO-based structural optimization method is developed to coordinate the design and performance improvement of the upper die and slider. The proposed approach incorporates multi-loading conditions and material distribution constraints to evaluate the responses of key components under different working scenarios. The objective of this study is to improve the lightweight level, durability, and stability of steel rolling dies.

The novelty of this study lies in developing, based on the conventional density-based TO framework, a unified optimization model for the complex service conditions of steel-rolling dies that integrates multiple constraints, including volume fraction, stress, deformation, and material distribution. Meanwhile, both impact loading and uniform static loading conditions are incorporated into a unified optimization framework, enabling coordinated structural design and performance optimization under multi-working conditions. In addition, the optimization scope is extended from a single component to the coordinated optimization of key components, namely the upper die and slider, achieving system-level structural optimization.

The main contributions of this study are as follows: a multi-constraint and multi-condition coordinated TO method for key components of steel-rolling dies is proposed. A multi-dimensional performance evaluation framework based on finite element simulation is established to systematically analyze mechanical response, energy absorption, thermal stability, and effectiveness. Furthermore, the proposed method for achieving coordinated improvement of structural lightweight design and performance is validated, providing practical guidance for mold structure design under complex working conditions.

2. Research Design

2.1. Construction of TO Algorithm based on Objective Function and Sensitivity Analysis

In the structural design of steel rolling molds, the stress distribution across various mold parts is complex, leading to issues such as low material utilization, local stress concentration, and potential fatigue risks. To optimize its structure, it is necessary to consider the overall force distribution of the structure, material volume fraction constraints, and stiffness requirements of key areas (Wentink et al. 2024). To achieve a reasonable layout of the structure while meeting requirements for material utilization and mechanical properties, it is necessary to quantify each unit's contribution to the overall performance. To clarify the optimization objective, the study minimizes structural flexibility to improve mold stiffness under the given material volume fraction constraint. The expression is shown in Eq. (1) (Yang et al. 2025).

$$\text{Minimize } f(\mathbf{x}) = \mathbf{U}^T \mathbf{K}(\mathbf{x}) \mathbf{U} \tag{1}$$

In Eq. (1), $\mathbf{x}$ represents the design variable vector and is the core variable in TO; $\mathbf{U}$ represents the structural displacement vector. $\mathbf{K}$ represents the strain energy of the structure. T represents transpose of displacement vector $\mathbf{U}$. $f(\mathbf{x})$ represents the flexibility index of the structure, used to evaluate the overall stiffness performance. In the optimization process, it is necessary to control the overall number of structural materials, and the constraint formula for material volume fraction is shown in Eq. (2).

$$\frac{\sum_{i=1}^{N}\rho_i v_i}{\sum_{i=1}^{N} v_i} \le V^* \tag{2}$$

In Eq. (2), N represents the total number of elements in the discretized finite element structure. v_i represents the volume of the i th unit. ρ_i represents the material density of the i th unit. V^* represents the total volume constraint allowed for materials. By using this constraint, the optimization process is ensured to be carried out under the premise of material conservation. The sensitivity calculation formula for each unit is shown in Eq. (3).

$$s_i = -\frac{\partial f}{\partial \rho_i} = \mathbf{U}_i^T \frac{\partial \mathbf{K}_i}{\partial \rho_i}\mathbf{U}_i \tag{3}$$

In Eq. (3), s_i represents the sensitivity of the i th unit to the objective function; ∂ stands for partial derivative. The sensitivity calculation formula is an important basis for updating design variables. To visually demonstrate the impact of sensitivity on topology design, this mechanism is visualized, and the results are shown in Fig. 1.

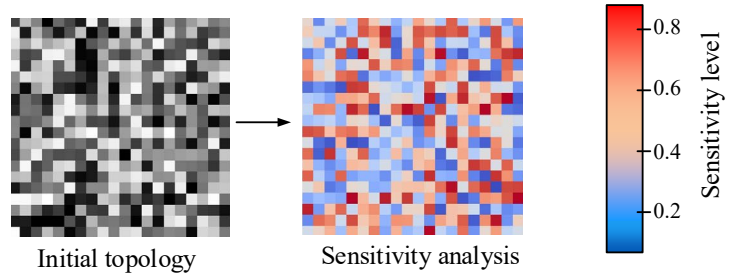

(a) Sensitivity heatmap

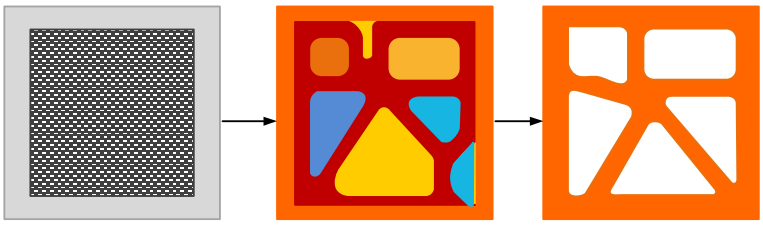

(b) Layout update visualization

Fig. 1. Sensitivity analysis and design variable update mechanism

Fig. 1(a) shows the visualized heatmap of the initial topology structure after sensitivity calculation. Fig. 1(b) shows the actual effect of this mechanism in topology layout updates. As shown in Fig. 1, the color from blue to red reflects the sensitivity level of each unit. Mapping the sensitivity of each unit in Fig. 1(a) onto the specific topology of Fig. 1(b), under the guidance of sensitivity analysis, the high sensitivity regions are preserved and strengthened after updating, while the low sensitivity regions are gradually removed, achieving effective coordination between structural performance and material usage. To truly transform the sensitivity analysis results into an iterative evolution of structural morphology, it is necessary to update and adjust the design variables of each unit based on the current sensitivity values. The update rule is shown in Eq. (4) (Herrmann et al. 2024).

$$\rho_i^{l+1} = \max(\rho_{\min}, \min(1, \rho_i^l - \alpha \frac{s_i - s_{\text{avg}}}{s_{\max} - s_{\min}})) \tag{4}$$

In Eq. (4), ρ_i^{l+1} represents the density of the i th unit in the $l+1$ th iteration. α represents the step size factor; s_{avg}, $s_{\max}$, and $s_{\min}$ represent the mean, maximum, and minimum sensitivity values, respectively. $\rho_{\min}$ represents the lower limit density of the material to avoid the occurrence of empty units. In the iterative process, to prevent numerical instability or checkerboard like phenomena, filtering processing is introduced (Platt et al. 2023). The specific expression is shown in Eq. (5).

$$\tilde{\rho}_i = \frac{\sum_{l \in A_i} \omega \rho_l}{\sum_{l \in A_i} \omega} \tag{5}$$

In Eq. (5), $\tilde{\rho}_i$ represents the filtered density. A_i represents the neighborhood of the i th unit. ω represents the filtering weight coefficient. By filtering, the continuity of material distribution can be ensured. To determine whether the optimization process converges, a threshold control standard for the magnitude of design variable changes is introduced, as shown in Eq. (6) (Cappellini et al. 2024).

$$\text{Converged if } \max_i \left|\rho_i^{l+1} - \rho_i^l\right| < \varepsilon \tag{6}$$

In Eq. (6), $\max_i$ represents taking the maximum value of the change in all units, which is used to measure the magnitude of the overall structural distribution change. ε represents the preset convergence threshold used to determine whether the design variable is stable. $\left|\rho_i^{l+1} - \rho_i^l\right|$ represents the change in the design variable of the i th unit between adjacent iterations. The above design variable update and convergence determination process constitute the complete TO iteration process, as shown in Fig. 2.

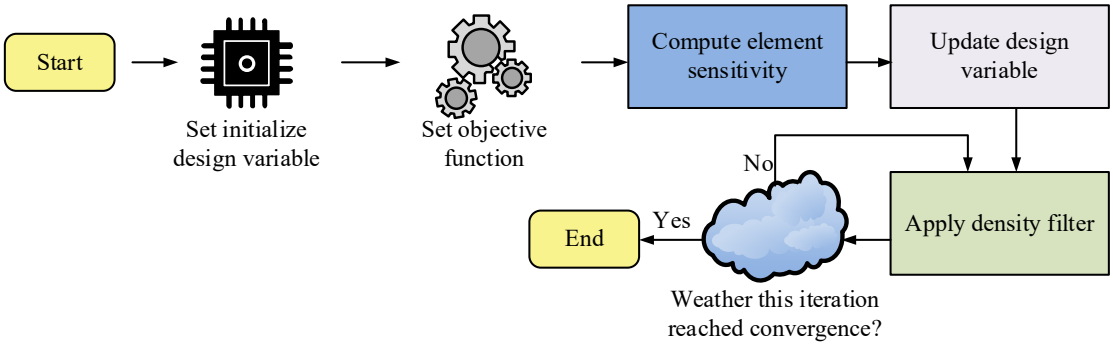

Fig. 2. Optimization iteration flowchart

As shown in Fig. 2, the optimized iterative process mechanism proposed in the study combines key modules, including sensitivity analysis of design variables, update control, and filtering constraints, to achieve efficient control of material distribution. First, the process starts with the initial layout and objective function, and it calculates sensitivity information for each unit based on the response analysis results to identify the sensitivity of material distribution to performance indicators. Second, design variables are updated based on sensitivity orientation, and weight filtering operations are introduced to suppress potential numerical oscillations and checkerboard patterns during the iteration process. After each round of design variable updates, the system will automatically perform a convergence judgment. If the density change of all units is less than the threshold, it is considered to have reached the convergence condition, and the optimization result is output. Otherwise, it will continue with a new iteration until the conditions are met, and the output result is obtained. Finally, the above objective function definition, constraint conditions, sensitivity analysis, and iterative process are integrated to form the overall structure of the TO algorithm, as shown in Fig. 3.

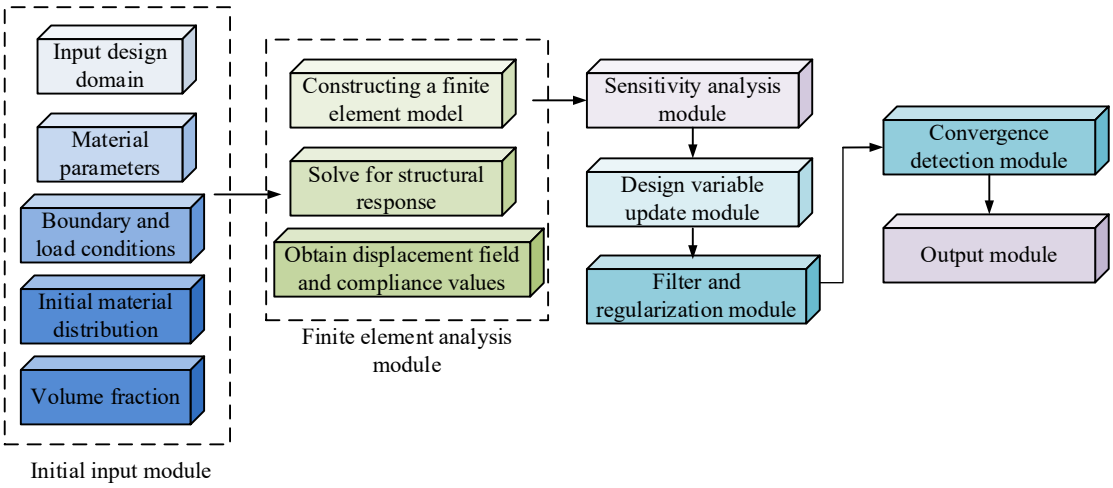

Fig. 3. Overall TO algorithm

As shown in Fig. 3, the overall TO algorithm comprises the following modules: initial input, finite element analysis, sensitivity analysis, design variable update, filtering and regularization, convergence determination, and output. First, the optimization direction and material dosage boundary are determined through the objective function and volume fraction constraints. Then, the design variables are updated based on the sensitivity calculation results to achieve gradual optimization of the structural distribution. To improve the continuity and manufacturing feasibility of the results, a filtering module is set

up to suppress checkerboard phenomena and numerical oscillations. Subsequently, the convergence determination module checks the magnitude of variable changes. When the set threshold is met, the result output is entered, and the iteration continues. The TO algorithm clarifies the functional positioning of each link within the overall optimization, providing a clear, operational execution path for controlled TO of complex structural components.

2.2. Optimization of the Upper Die and Sliding Block of the Steel Rolling Die

After completing the overall construction of TO algorithms and clarifying the performance constraint mechanism, further research will be conducted on the optimization design of key components in steel rolling dies. In actual steel rolling operations, the upper die and slider are the most complex and vulnerable core components in the mold system. The upper die determines the overall sealing and force balance of the molding, while the slider undertakes the composite functions of guidance, clamping, and molding boundary control. If the structural design of the two is unreasonable, it will not only shorten the life of the mold and waste materials, but may also cause serious working conditions, such as mold fatigue fracture and stamping errors. Therefore, the study establishes TO models for these two key modules separately and introduces a unified performance constraint mechanism to improve the overall load-bearing stability, lightweight level, and manufacturing adaptability of the mold. The original structure of each component of the steel-rolling die used for optimization is shown in Fig. 4.

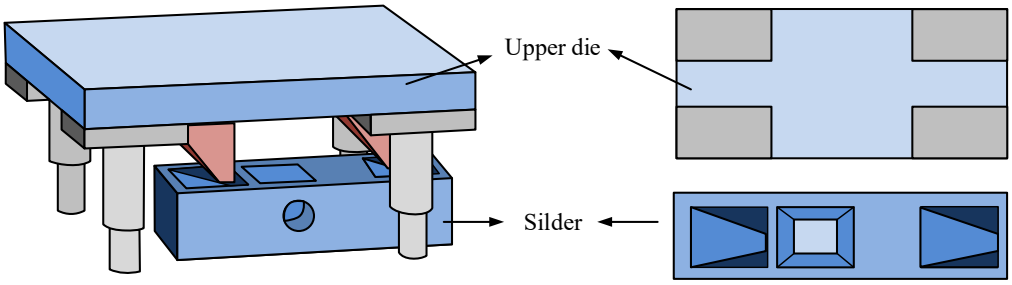

(a) 3D diagram (b) Top view

Fig. 4. Initial structures of upper die and slider

In Fig. 4, the two core structural modules selected by the research are the upper die and the slider. In the 3D structural view on the left, the upper die is placed on the top layer of the mold, with four convex modules arranged inside for forming. The slider is in the middle position, forming a support loop with the mold base and containing three rectangular through-holes for material flow and discharge. At present, although the structure has basic forming functions, the thick upper die section and the large solid part of the slider create significant redundancy. There is structural and functional overlap, and multiple areas inside the slider have not participated in the actual forming operation, forming an idle structure. Overall, the initial structure urgently needs to be optimized through topology methods to eliminate inefficient areas, streamline structural volume, and improve mold performance and engineering adaptability while ensuring strength and stiffness requirements. For the upper die part, combined with the processing and installation boundary, the set constraint conditions are set as shown in Eq. (7) (Lu et al. 2025).

$$g_1(\rho) = \frac{1}{V_0}\int_\Omega \rho(x)\mathrm{d}x - V^* \tag{7}$$

In Eq. (7), $g_1(\rho)$ represents the constraint function. V_0 represents the total volume of the design area. Ω represents the structural design area. To further improve the performance of the structure under stress, the study introduces stress analysis formulas to constrain key parts of the upper die. The calculation formula is shown in Eq. (8).

$$g_2(\rho) = \sigma_{\max}(\rho) - \sigma_{\text{allow}} \tag{8}$$

In Eq. (8), $g_2(\rho)$ represents the stress constraint function of the structure under the current density distribution. $\sigma_{\max}(\rho)$ represents the maximum equivalent stress of the optimized structure under loading conditions. σ_{allow} represents the upper limit of allowable stress for the material. To accurately capture the response behavior of the slider during the loading process, a deformation control model for the slider is introduced. Its mathematical expression is shown in Eq. (9).

$$g_3(\rho) = \delta_{\max}(\rho) - \delta_{\text{limit}} \tag{9}$$

In Eq. (9), $g_3(\rho)$ represents the constraint expression for the maximum deformation of the block structure. $\delta_{\max}(\rho)$ represents the maximum displacement response of the structure under the current design variable distribution. δ_{limit} represents the preset maximum allowable deformation limit. This formula is used to control the structure's deformation, ensuring that the slider's deformation after loading does not exceed its functional limit. The study adopts an overall objective function to integrate the above multiple constraints into a unified objective framework, as defined in Eq. (10).

$$f(\rho) = c(\rho) + \lambda_1 \cdot g_1(\rho)^2 + \lambda_2 \cdot g_2(\rho)^2 + \lambda_3 \cdot g_3(\rho)^2 \tag{10}$$

In Eq. (10), $f(\rho)$ represents the total objective function value. $c(\rho)$ represents the flexibility function, which refers to the flexible response of the structure under a given load. λ_1, λ_2, and λ_3 represent the penalty factors for volume fraction, stress, and deformation constraints, respectively. In addition, to ensure the material adaptability of the obtained structure during manufacturing and service, material mechanical property constraints also need to be considered. The constraint function is shown in Eq. (11).

$$g_4(\rho) = \mathrm{Var}(E(\rho)) - \theta \tag{11}$$

In Eq. (11), $g_4(\rho)$ represents the variance constraint function of the elastic modulus distribution of the material; $\mathrm{Var}(E(\rho))$ represents the statistical variance of the elastic modulus of each unit in the structure; θ represents the maximum allowable variance limit for material performance distribution. This constraint helps to control the uniformity of materials in various regions and improve the controllability of manufacturing processes. Ultimately, to quantify the overall performance of the system, performance evaluation indicators are further introduced. Its expression is shown in Eq. (12).

$$\eta = \frac{W_{\mathrm{opt}}}{W_{\mathrm{init}}} \cdot \frac{C_{\mathrm{init}}}{C_{\mathrm{opt}}} \tag{12}$$

In Eq. (12), η represents the comprehensive performance evaluation value of the structure. W_{opt} and W_{init} respectively represent the quality of the optimized and initial structures. C_{opt} and C_{init} represent the flexibility indicators of the optimized and initial structures, respectively. Finally, the optimized upper die and slider structures of the steel rolling die are shown in Fig. 5.

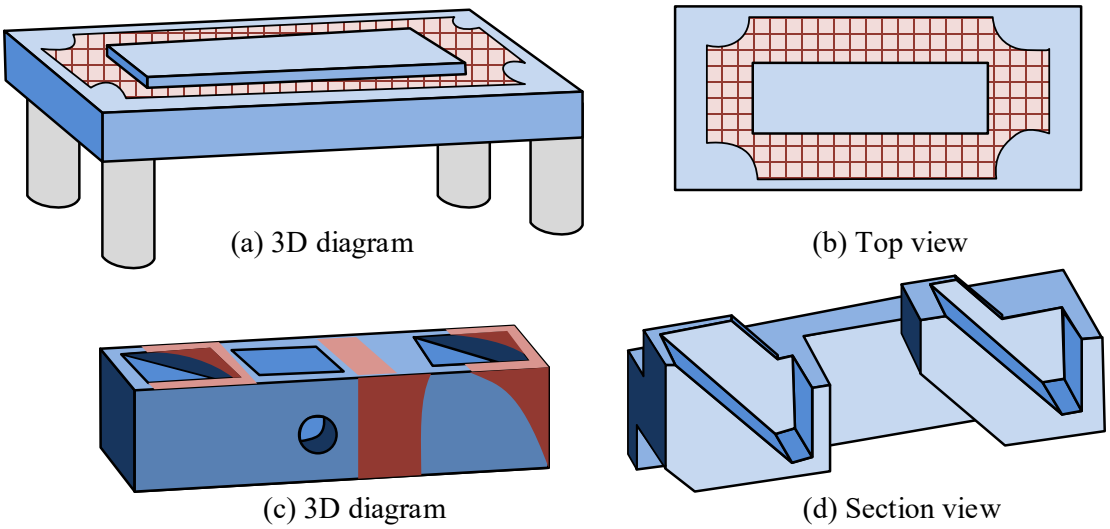

Fig. 5. Optimized structure of upper die

Figs. 5(a) and 5(b) show the optimized design of the upper die, while Figs. 5(c) and 5(d) show the optimized design of the slider. In Figs. 5(a) and 5 (b), the parts marked by the grid in the Fig. are the structures that have been optimized and removed. The optimized upper die effectively removes a large amount of non-load bearing materials in the central solid area, forming a more reasonable distribution of reinforcement ribs, while retaining key support parts connected to the guide column and punch, ensuring structural stability while minimizing weight. In Figs. 5(c) and 5(d), many redundant areas in the original slider that did not participate in the main force transmission have been removed, forming a more compact and efficient internal support system. In terms of structural preservation, the key functional features of the slider, such as positioning holes, installation holes, and transmission interfaces, are fully preserved and reinforced in the surrounding area to ensure that the accuracy of the fit with other mold components is not affected. The overall structure significantly reduces material volume and processing burden while maintaining sufficient strength and stiffness, improving material utilization efficiency.

3. Results

3.1. TO Algorithm Parameter Testing and Performance Comparison Before and After Mold Optimization

To meet the requirements of finite element simulation accuracy and iterative solving efficiency for the TO steel-rolling die structure, a targeted experimental operating environment was established. The hardware platform was based on the Intel Core i9-13900K high-performance multi-core processor, combined with 128GB DDR5 memory and NVIDIA RTX 4090 graphics card, fully ensuring the convergence computational efficiency of large-scale structural models in multiple iterations and high-dimensional variable spaces. In terms of software environment, the optimization model was developed using MATLAB R2023b as the core platform, and its built-in optimization and matrix operation toolbox was called to execute the

main iteration process. Finite element analysis was performed using ANSYS Mechanical 2023 R1 to determine physical quantities, such as the stress and displacement fields. The study first selected two key hyperparameters, step size factor α and filtering weight coefficient ω, from TO algorithms for value selection testing. Flexibility was used as a performance evaluation indicator, and its trend with the number of iterations was tested to determine the optimal hyperparameter combination. The test results are shown in Fig. 6.

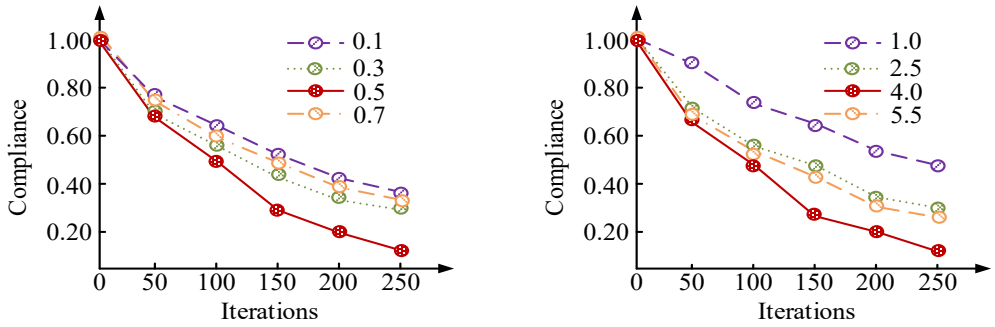

(a) Step size factor (b) Filter weight

Fig. 6. Parameter selection tests for the TO algorithm

Fig. 6(a) shows the selection test results of the step size factor α, and Fig. 6(b) shows the selection test results of the filtering weight coefficient ω. As shown in Fig. 6(a), with the increase of α value, the rate of decrease in flexibility during the optimization process accelerated. When α=0.5, the flexibility of each iteration stage was at its lowest level. After 250 iterations, it converged to 0.105, which was better than the final convergence value of 0.361 when α=0.1 and 0.337 when α=0.7. As shown in Fig. 6(b), when ω=4.0, the flexibility values at each iteration stage were better than those for other parameter configurations and ultimately converged to 0.107. When ω=1.0 and 2.5, although the decrease was significant in the early stage, it tended to plateau in the middle and later stages, and the final flexibility values remained at 0.466 and 0.314. Therefore, the study determined the optimal parameter combination as α=0.5 and ω=4.0, which exhibited the best convergence speed and flexibility performance. After determining the optimal hyperparameter combination, further comparisons were made between the optimization effects of the upper die and slider on key performance parameters such as structural mass, volume, maximum stress, and maximum displacement. The relevant results are shown in Fig. 7.

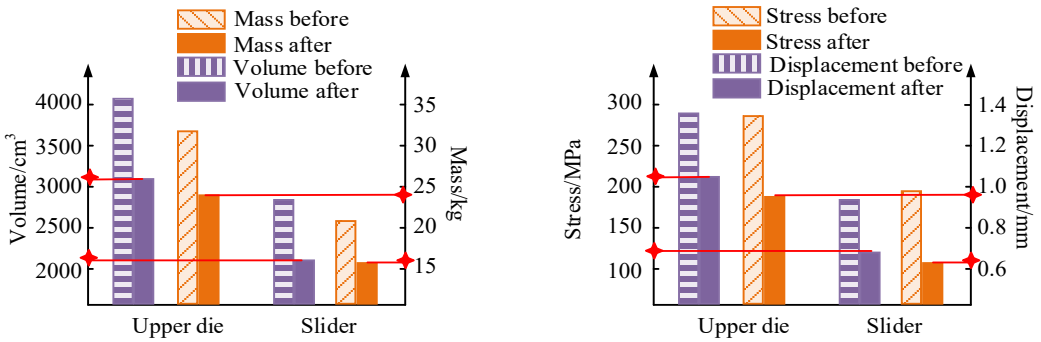

(a) Comparison of mass and volume (b) Comparison of max stress and max displacement

Fig. 7. Overall comparison of structural performance before and after optimization

Fig. 7(a) shows the comparison results of the mass and volume structural indicators of the upper die and slider before and after optimization, and Fig. 7(b) shows the changes in the maximum equivalent stress and maximum displacement. According to Fig. 7(a), after TO, the mass of the upper die decreased from 32.7 kg to 24.1 kg, and the volume decreased from 4100 cm³ to 3020 cm³; The mass and volume of the slider have decreased by 23.9% and 23.8% respectively. As shown in Fig. 7(b), the maximum equivalent stress of the upper die decreased from 294.3 MPa to 218.5 MPa, and the maximum displacement decreased from 1.34 mm to 0.91 mm. The maximum equivalent stress of the slider decreased from 185.6 MPa to 127.2 MPa, and the maximum displacement decreased from 0.96 mm to 0.63 mm. Overall, the upper die and slider achieved comprehensive improvement in load response performance while reducing mass, verifying the effectiveness of the optimization method in balancing structural lightweighting and mechanical strengthening in this study. On this basis, the study further evaluated the other three key structural performance indicators, and their comparison is shown in Table 1.

According to Table 1, after optimization, the dynamic response times of the upper die and slider decreased from 0.014 s and 0.018 s to 0.010 s and 0.012 s, respectively, resulting in a response speed increase of over 28%. In terms of thermal stability, the temperature of the upper die and slider decreased by 12.2% and 14.0%, respectively. The safety margin has been significantly improved, with the upper die increasing from 1.44 to 1.83 and the slider increasing from 1.39 to 1.77, both

by over 27%. This data indicates that structural optimization has improved mold performance and achieved significant improvements in responsiveness and safety.

Table 1. Comparison of different performance metrics before and after optimization

Component	Optimization	Dynamic responsiveness/s	Thermal stability/℃	Safety margin
Upper die	Before	0.014	62.4	1.44
	After	0.010	54.8	1.83
Slider	Before	0.018	65.1	1.39
	After	0.012	56.0	1.77

3.2. Structural Performance Testing of Upper Die and Slider

To evaluate the mechanical performance of optimized structures under various practical working conditions, a simulation environment based on the finite element method was developed. The simulation process used ANSYS Workbench 2022 R2 as the main modeling and analysis platform and utilized its Static Structural module for static analysis. Two typical working conditions were designed to simulate the force characteristics at different processing stages. Condition 1 simulated the initial rolling stage, with the loading point at the end of the slider to simulate the impact load. Condition 2 simulated the steady-state rolling stage, with the loading point at the center of the upper die and a uniform static load applied. The material parameters were uniformly set to 45 steel (density 7.85g/cm^3, elastic modulus 210GPa, Poisson's ratio 0.3). The mesh was generated using an automatic local refinement strategy, with the element sizes controlled within 3mm to balance computational accuracy and efficiency. To verify mesh independence, a comparative analysis with different mesh sizes was conducted. When the element size decreased from 5mm to 3mm, the variation in key performance indicators (maximum equivalent stress and displacement) was less than 3%, indicating that the results are insensitive to mesh refinement. Considering both accuracy and computational cost, a mesh size of 3mm was adopted. To evaluate the thermal response of the optimized structure, temperature evolution under the two typical loading conditions was simulated. In the thermal analysis, the material was assumed to have isotropic and temperature-independent thermal properties, and radiative heat transfer was neglected. Only heat conduction and convective heat transfer were considered, with a constant convection coefficient applied as the boundary condition to ensure computational stability. Fig. 8 shows the temperature variation over time. The trend in temperature with running time is shown in Fig. 8.

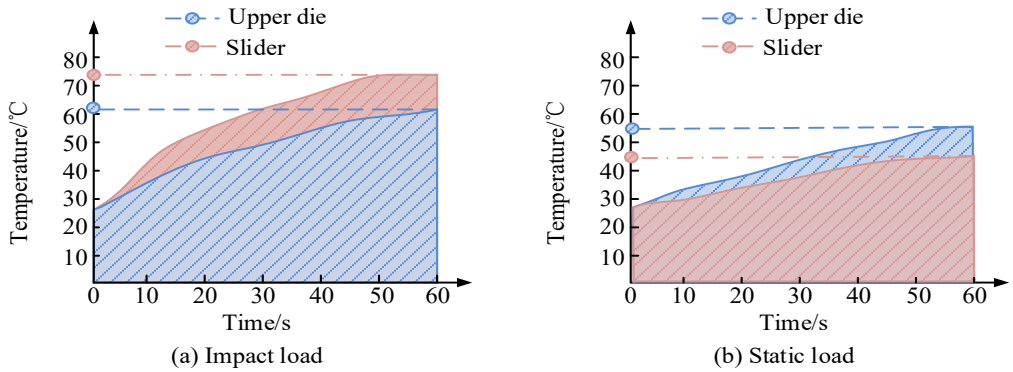

Fig. 8. Thermal response of optimized upper die and slider under two load conditions

Fig. 8(a) shows the temperature variation trend of the optimized upper die and slider center over time under impact load conditions, while Fig. 8(b) shows the temperature variation trend under uniform static load conditions. According to Fig. 8(a), under impact load conditions, the temperature of the slider rapidly increased from the initial 28.0 ℃ to 76.3 ℃, and the temperature of the upper die rose to 60.2 ℃. The heating rate was fast in the first 30 seconds and tended to plateau in the later stage, indicating that the structure has a strong ability to withstand instantaneous thermal shock under this working condition. Fig. 8(b) shows that under steady-state static load conditions, the temperature rise of the upper die and slider was controlled within 54.1 ℃ and 44.0 ℃, respectively, and the temperature changes were more stable. Overall, there were no significant temperature changes or local overheating phenomena observed in the structures under the two types of working conditions. This result confirms that the optimized structure exhibits strong thermal adaptability and stability, meeting the service requirements of mold components subjected to high-frequency cyclic loads. The study conducted simulation tests on the upper die and slider under two types of operating conditions before and after optimization, using the maximum equivalent stress as the indicator. The results are shown in Fig. 9.

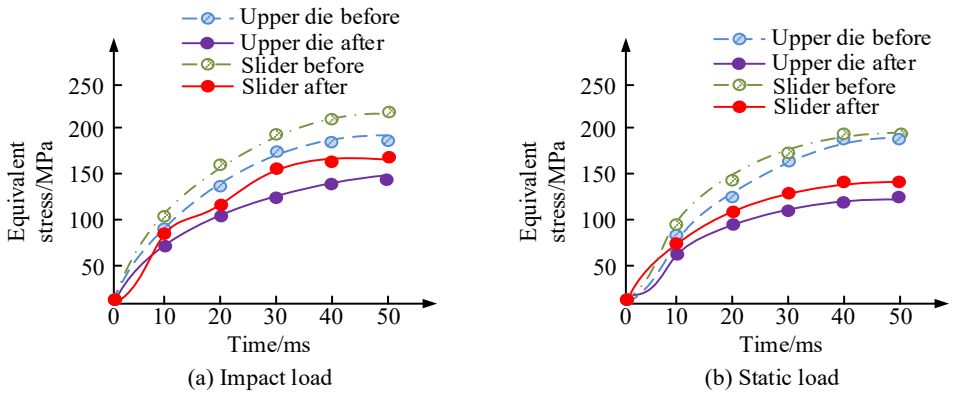

Fig. 9. Equivalent stress evolution curves of upper die and slider under two load conditions

Fig. 9(a) shows the trend in the maximum equivalent stress of the upper die and slider before and after optimization over time under impact load conditions. Fig. 9(b) shows the trend of maximum equivalent stress variation under uniform static load conditions. According to Fig. 9(a), under the action of impact load, the stress of the upper die before optimization was 193.6 MPa at 50ms, and after optimization, it decreased to 145.9 MPa, a decrease of 24.7%. The slider decreased from 221.3 MPa to 167.2 MPa, a decrease of 24.4%. Fig. 9(b) shows that under uniform static load conditions, the stress on the upper die and slider decreased from 184.2 MPa and 193.3 MPa to 130.1 MPa and 146.5 MPa, respectively, at 50ms. From this, TO can effectively suppress the stress response of key structures under different working conditions, enhancing the structural load-bearing stability and service safety. The study continued to compare and analyze the optimization effects of the upper die and the slider on energy absorption per unit mass, as shown in Fig. 10.

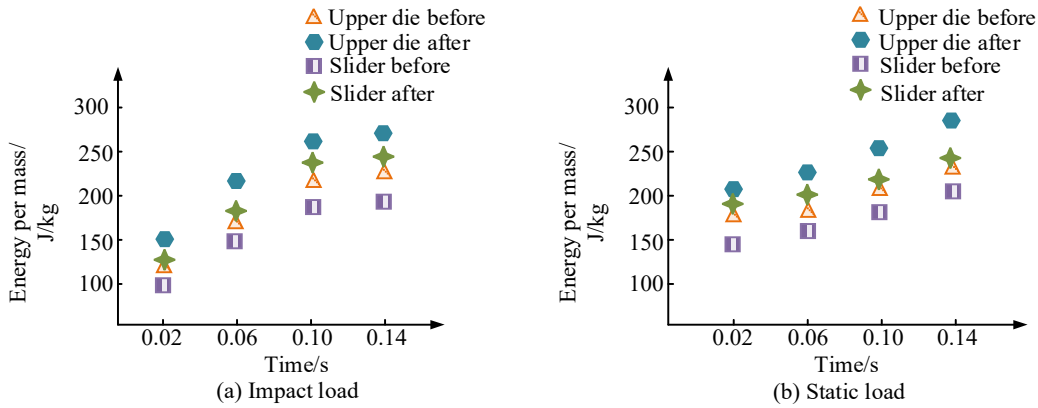

Fig. 10. Comparison of specific energy absorption under two load conditions

Fig. 10(a) shows the trend of the absorption energy per unit mass of the upper die and slider before and after optimization over time under impact load. Fig. 10(b) shows the variation of similar performance indicators under uniform static load conditions. According to Fig. 10(a), at 0.14s, the absorption energy per unit mass of the upper die increased from 241 J/kg before optimization to 278 J/kg, an increase of 15.4%. The slider increased by approximately 21.1%. Fig. 10(b) showed that under uniform static load, the absorption energy per unit mass of the upper die and slider increased to 276 J/kg and 247 J/kg, respectively. The proposed optimization strategy effectively improved the impact resistance and comprehensive toughness of the components. To further verify the applicability of the optimization scheme to multidimensional performance indicators, the study continued by comparing and analyzing its performance under additional simulation parameters, as shown in Table 2.

According to Table 2, under impact load conditions, the natural frequencies of the upper die and slider increased from 312.5 Hz and 276.3 Hz to 346.8 Hz and 310.6 Hz, respectively, an increase of over 11%. Under uniform static load, the frequencies of both increased synchronously by over 12%, indicating a significant enhancement in structural stiffness. In terms of energy dissipation ratio, the optimized upper die and slider achieved about a 5% improvement in both operating conditions, reflecting their enhanced ability to absorb energy and mitigate impacts. In terms of the deformation uniformity index, the upper modulus increased from 0.63 to 0.81, and the slider increased from 0.57 to 0.76. The simulation results for this multidimensional indicator show that after optimization, the overall force distribution is more balanced, structural deformation is more coordinated, and the service stability of the steel rolling die is further improved.

Table 2. Performance comparison under two load conditions

Condition	Component	Optimization	Natural frequency/Hz	Energy dissipation/%	Deformation uniformity index
Impact load	Upper die	Before	312.5	18.4	0.63
		After	346.8	23.7	0.81
	Slider	Before	276.3	16.9	0.57
		After	310.6	21.6	0.76
Static load	Upper die	Before	298.1	15.2	0.59
		After	335.4	20.3	0.79
	Slider	Before	261.2	14.6	0.53
		After	294.5	19.1	0.74

4. Conclusion

To address the issues of structural redundancy and delayed energy dissipation in steel rolling dies under complex working conditions, a TO-based structural design method with coordinated lightweight and performance enhancement is proposed. The method adopts compliance minimization as the objective function and establishes an optimization model that balances structural responsiveness and stability. A coordinated optimization is conducted for the key components, namely the upper die and slider. Based on finite element simulation results, the optimized structure shows improvements across multiple performance indicators. Specifically, the average mass and volume are reduced by more than 25%, while the maximum stress and displacement decrease by approximately 23.9% to 29.4%. In terms of energy absorption, the specific energy absorption of the upper die and slider increases to 278 J/kg and 253 J/kg, respectively. Additionally, the natural frequency, energy dissipation rate, and deformation uniformity are all enhanced to varying degrees. These results indicate that the optimized structure exhibits improved load response capability and stability under multi-loading conditions. From an engineering application perspective, the proposed method provides a useful reference for the structural design and optimization of key components in steel rolling dies, particularly for lightweight design under complex multi-loading conditions. By introducing a multi-constraint TO mechanism at the design stage, material utilization can be improved, and stress distribution can be optimized, thereby providing a solid performance foundation for subsequent manufacturing and operation. Furthermore, from a managerial and decision-making perspective, the proposed method offers a quantitative basis for design and manufacturing processes. During the product development stage, reliance on experience-based design can be reduced by prioritizing multi-constraint optimization strategies to enhance structural performance. Under multi-condition operating scenarios, simulation-based results can guide targeted optimization of key components, thereby reducing the risk of structural failure. In terms of cost control, this method helps reduce material redundancy and improve resource utilization efficiency. However, in practical applications, further considerations such as manufacturing constraints, material nonlinear behavior, and uncertainties in service conditions are required to refine and validate the optimization results. It should be noted that the findings of this study are primarily based on numerical simulations and lack experimental validation. In addition, from a theoretical standpoint, the proposed approach is built upon the conventional density-based TO framework and does not introduce fundamental theoretical advancements. Future work will focus on extending the method by incorporating multi-physics coupling, nonlinear behavior modeling, and manufacturability constraints to enhance both theoretical depth and engineering applicability.

Funding

This research received no specific financial support from any funding agency.

Institutional Review Board Statement

Not applicable.

Declaration of Artificial Intelligence (AI) Tools

The author confirms that no AI tools were used in the preparation of this manuscript.

References

Asadi, M., Poursina, M., Pourfarid, S., and Aboutalebi, F. H. (2023). Optimization of reduction schedule in a tandem cold rolling mill considering the material properties of the strip. *International Journal of Material Forming, 16*(3), 2829. https://doi.org/10.1007/s12289-023-01751-6

Banh, T. T., and Lee, D. (2024). Comprehensive polygonal topology optimization for triplet thermo-mechanical-pressure multi-material systems. *Engineering with Computers, 40*(5), 3295-3317. https://doi.org/10.1007/s00366-024-01982-4

Cappellini, C., and Giorleo, L. (2024). Ring rolling with flat dies: An analytical method to optimize geometry, time or energy. *Journal of Mechanical Science and Technology, 38*(10), 5543-5558. https://doi.org/10.1007/s12206-024-0926-y

Chen, Y., Peng, L., and Feng, P. (2023). Optimization of multi-segment work roll profile for 1340 mm HC tandem cold-rolling mills based on DBSCAN and NSGA-II algorithms. *Steel Research International, 94*(11), 2300-2307. https://doi.org/10.1002/srin.202300077

Elmoghazy, Y., Abuelgasim, E. M. O., and Osman, S. A. (2023). Effective mechanical properties evaluation of unidirectional and bidirectional composites using virtual domain approach at microscale. *Archives of Advanced Engineering Science, 1*(1), 27-37. https://doi.org/10.47852/bonviewAAES32021723

Frederiksen, A. H., Sigmund, O., and Poulios, K. (2024). Topology optimization of self-contacting structures. *Computational Mechanics, 73*(4), 967-981. https://doi.org/10.1007/s00466-023-02396-7

Gao, F., Fang, Q., Zha, W., Huang, L., Li, X., Zhang, H., and Ni, H. (2024). Optimization of multiphase flow and initial solidification behaviors in a stainless steel mold by SEN design. *Metallurgical and Materials Transactions B, 55*(4), 2717-2731. https://doi.org/10.1007/s11663-024-03135-w

Herrmann, M., Kazempour, D., and Scheipl, F. (2024). Enhancing cluster analysis via topological manifold learning. *Data Mining and Knowledge Discovery, 38*(3), 840-887. https://doi.org/10.1007/s10618-023-00980-2

Hu, Y., Zhang, Y., Ma, X., Du, X., Wang, W., and Zhang, H. (2024). Virtual commissioning and process parameter optimization of rolling mill based on digital twin. *The International Journal of Advanced Manufacturing Technology, 130*(1), 705-716. https://doi.org/10.1007/s00170-023-12718-x

Li, Y., Ma, B., Zheng, J., Zhu, J., and Lei, G. (2023). Electromagnetic and mechanical topology optimization for SynRM rotors considering high dimensional constraints. *IEEE Transactions on Industrial Electronics, 70*(12), 12048-12059. https://doi.org/10.1109/TIE.2023.3234146

Lu, Y., and Zhou, M. (2025). Structural topology optimization for crash intrusion control under contact. *Structural and Multidisciplinary Optimization, 68*(8), 1-24. https://doi.org/10.1007/s00158-025-04086-9

Ooms, T., Vantyghem, G., Thienpont, T., Coile, R., and Corte, W. (2023). Compliance-based topology optimization of structural components subjected to thermo-mechanical loading. *Structural and Multidisciplinary Optimization, 66*(6), 126-127. https://doi.org/10.1007/s00158-023-03563-3

Patwari, A. U., Bhuiyan, S. A., Noman, K., and Navid, W. (2024). Defects and remedies in casting processes: A combinatorial approach between manual and digital optimization technique for enhanced quality casting. *Discover Mechanical Engineering, 3*(1), 39-40. https://doi.org/10.1007/s44245-024-00067-2

Platt, T., Baumann, J., and Biermann, D. (2023). Potential of high-feed milling structured dies for material flow control in hot forming. *Production Engineering, 17*(3), 463-471. https://doi.org/10.1007/s11740-022-01165-4

Wang, Y., and Sigmund, O. (2024). Topology optimization of multi-material active structures to reduce energy consumption and carbon footprint. *Structural and Multidisciplinary Optimization, 67*(1), 5-7. https://doi.org/10.1007/s00158-023-03698-3

Wentink, D. J., and Schutte, K. (2024). Wear of cylinders in tractive rolling contact and implications for modelling back up roll wear in steel cold rolling mills. *BHM Berg- und Hüttenmännische Monatshefte, 169*(11), 607-611. https://doi.org/10.1007/s00501-024-01525-w

Yang, C., Wang, Q., and Lu, W. (2025). Integrated uncertain optimal design strategy for truss configuration and attitude–vibration control in rigid–flexible coupling structure with interval uncertainties. *Nonlinear Dynamics, 113*(3), 2215-2238. https://doi.org/10.1007/s11071-024-10291-w

You, L., Yao, L., Li, X., Jia, G., and Lv, G. (2023). Numerical simulation and casting process optimization of cast steel node. *The International Journal of Advanced Manufacturing Technology, 126*(11), 5215-5225. https://doi.org/10.1007/s00170-023-11460-8

Zhang, Y., Lin, R., Zhang, H., and Peng, Y. (2023). Vibration prediction and analysis of strip rolling mill based on XGBoost and Bayesian optimization. *Complex & Intelligent Systems, 9*(1), 133-145. https://doi.org/10.1007/s40747-022-00795-6

Zong, H., Zhang, J., and Jiang, L. (2024). Bionic lightweight design of limb leg units for hydraulic quadruped robots by additive manufacturing and topology optimization. *Bio-Design and Manufacturing, 7*(1), 1-13. https://doi.org/10.1007/s42242-023-00256-0

Tao Chen obtained a master's degree in engineering in 2013. Currently, he serves as an Associate Professor at the School of Mechanical and Automotive Engineering, Sanmenxia Vocational and Technical College. His research interests include mold design and manufacturing, applications of 3D scanning technology, and applications of 3D printing.